Supporting Information

Veyrac et al. 10.1073/pnas.1220558110

SI Methods

Animals. Adult (2–3 mo old) male *zif268* homozygous knockout mice (*zif268*-KO, $n = 70$), heterozygous (*zif268*-HET, $n = 5$) and WT ($n = 68$) littermate mice, generated as described previously (1) and backcrossed onto a C57BL/6J background for 24 generations, were used in this study. The mice were housed in a temperature and light-controlled colony room (12-h light/dark cycle) in groups of three per cage with dry food and water ad libitum. Experiments were conducted during light phase and were performed blind to genotype. All efforts were made to minimize the number of animals and their suffering during the experiments, conducted in accordance with the European Communities Council Directive 86/609/EEC and the French National Committee (87/848).

BrdU Administration. To study proliferation, mice (WT $n = 7$, *zif268*-KO $n = 7$) received one intraperitoneal injection of BrdU (50 mg/kg in 0.9% NaCl; Sigma-Aldrich) and were killed 4 h later. For cell survival, mice were given five BrdU injections (50 mg/kg) at 2-h intervals on a single day and were killed 7 (WT $n = 7$, *zif268*-KO $n = 8$), 14 (WT $n = 8$, *zif268*-KO $n = 8$), 21 (WT $n = 6$, *zif268*-KO $n = 7$), and 28 (WT $n = 7$, *zif268*-KO $n = 7$) d later. Five heterozygous mice were also used to examine neurogenesis 21 d after BrdU injections. For behavioral experiments, mice (WT $n = 28$, *zif268*-KO $n = 26$) were injected with three intraperitoneal injections of BrdU (100 mg/kg) at 4-h intervals and trained 9 or 18 d after in a Morris water-maze task.

Morris Water-Maze Set-Up and Training Procedures. The apparatus consisted of a circular pool (150 cm in diameter, 37 cm high) filled with water (20 °C ± 0.5 °C) made opaque by adding a white, nontoxic opacifier (Acusol OP301 Opacifier; Rohm and Haas). White curtains affixed with large extramaze visual cues surrounded the pool, which was divided into four virtual quadrants. The platform (11.5 cm in diameter) was located in the center of one quadrant (i.e., target quadrant) and remained at a fixed location during training. The three other quadrants served as starting points, assigned pseudorandomly and varied on every trial. Mice were handled each day for a week to get used to the experimenter. The day before training, mice were submitted to a single familiarization block of three trials, with the platform protruding 0.5 cm above the water surface. The maximal duration for each trial was 60 s. Mice failing to find the platform were gently guided to it and allowed to remain on it for 60 s before being replaced in the water from another starting point. The next day, mice were trained to locate the hidden platform submerged 0.5-cm below the water surface. The massed-training procedure consisted in two training sessions separated by 4 h, each composed of four blocks, 20-min apart, of three consecutive trials (2). Mice were trained in the water maze 9 d (WT $n = 6$, *zif268*-KO $n = 6$) or 18 d (WT $n = 10$, *zif268*-KO $n = 8$) after BrdU injections and were tested for long-term memory 25 d later in one or two probe tests held without platform. Because mice injected with BrdU 9 or 18 d before training did not show any statistical difference in learning performance, data were pooled (WT: $F_{1,14} = 0.55$, group $P = 0.47$; time $P < 0.0001$; interaction $P = 0.89$; KO: $F_{1,12} = 0.52$, group $P = 0.48$; time $P < 0.0001$; interaction $P = 0.25$).

Control groups consisted of undistributed mice remaining in their home cages, handled twice a week and killed 34 d (WT $n = 6$, *zif268*-KO $n = 6$) or 43 d (WT $n = 6$, *zif268*-KO $n = 6$) after BrdU injections. We did not add Swim groups in this study because it was previously shown that this training procedure induced the same level of long-term survival of newborn neurons in Swim and Cage controls (2). A video-tracking software (ANY-maze; Stoelting) was used for automatic recording of the latency to find the platform, swim speed and path lengths, and activity in a 19-cm width virtual corridor set along the wall (thigmotaxis). Data were averaged per blocks of trials and statistically tested by a two-way ANOVA. During probe tests, the time spent in each quadrant of the pool and the number of crossings over the platform position were recorded. Data were analyzed with one-sample *t* test relative to 25% and Student *t* test between WT and KO mice. Mice were killed 90 min after the probe test.

Stereotaxic Injection. Engineered self-inactivating Moloney murine retroviruses expressing GFP to label proliferating cells and their progeny were used (3). Z*if268*-KO ($n = 7$) and WT ($n = 7$) littermate mice housed under standard conditions were stereotaxically injected with the retroviral solution in the dentate gyrus (DG) (1 μL at 0.2 μL/min) at coordinates −1.7 mm from bregma, ±1.7 mm lateral, 1.7 mm below brain surface. Mice were killed 3 (WT $n = 3$; *zif268*-KO $n = 3$) and 6 wk (WT $n = 4$; *zif268*-KO $n = 4$) later.

Tissue Preparation and Sectioning. Mice were deeply anesthetized with pentobarbital (0.2 mL/30 g body weight) and perfused transcardially with a solution containing 4% (vol/vol) cold paraformaldehyde in 0.1 M phosphate buffer (PB), pH 7.4. Brains were dissected out and fixed overnight in the same perfusion solution at 4 °C, immersed for 5 d in PB containing 20% sucrose and frozen in chilled 2-methylbutane (−50 °C). Coronal serial sections [14-μm thick for the DG and 40-μm thick for olafactory bulb (OB) and subventricular zone (SVZ)] were cut with a cryostat (Microm HM 550 OMP). Sections of 14-μm thick were mounted on superfrost-plus slides (Techno Scientific). For the retrovirus injection groups, brains were cut in 60-μm-thick free-floating sections at the same anatomical levels.

Immunochemistry. As described previously (4), brain sections were preincubated in Target Retrieval Solution (Dako) for 20 min at 95 °C. After cooling for 20 min, sections were treated with 0.5% Triton in PBS for 30 min and then for 3 min with pepsin (0.0125% in 0.1 N HCl; Sigma-Aldrich). Endogenous peroxidases were blocked with a solution of 3% H_2O_2 in 0.1 M PBS. Sections were then incubated for 90 min in 5% normal serum (Jackson Immunoresearch), 5% BSA (Sigma-Aldrich), and 0.125% Triton X-100 to block nonspecific binding, and incubated overnight at 4 °C in a mouse anti-BrdU primary antibody (1:100; Millipore) to label newborn cells, or a rabbit anti-Zif268 or rabbit anti–c-Fos antibody to label activated cells. Sections were then incubated in a horse biotinylated anti-mouse (1:200; Vector Laboratories) or a goat biotinylated anti-rabbit (1:200; Vector Laboratories) secondary antibody for 2 h at room temperature. Sections were then processed with avidin-biotin-peroxydase complex (1:200; ABC Elite Kit; Vector Laboratories) for 30 min, followed by three rinses of 5 min in PBS. Finally, peroxidase detection was conducted with 3,3-diaminobenzidine-tetrahydrochloride (0.06%; Sigma-Aldrich) as chromogen with nickel (0.03% $NiCl_2$) and H_2O_2 (0.03%) to obtain black immunolabeling. Sections were dehydrated in graded ethanols and coverslipped in Eukitt (Sigma-Aldrich).

For BrdU double- and triple-labeling, sections treated as above were incubated overnight at 25 °C in rat anti-BrdU (1:100; Abcys) or mouse anti-BrdU (1:100; Millipore) antibodies with guinea-pig antidoublecortin (anti-DCX) (1:500; Millipore), mouse anti-NeuN (1:500; Millipore), rabbit anti-GFAP (1:3,000; DAKO), rabbit anti-Zif268 (1:1,000; Santa Cruz Biotechnology), rabbit

anti–c-Fos (1:3,000; Santa Cruz), rabbit anti-adenylate cyclase III (ACIII; 1:250; Santa Cruz), rabbit anti-glutamate receptor 1 (GluR1; 1:200; Millipore), rabbit anti-KCC2b (1:500; Sigma-Aldrich), or mouse anti-NKCC1 (1:200; T4-c; DSHB) antibodies. Sections were then incubated for 2 h at room temperature in goat anti-rat Alexa 568 (1:200; Invitrogen) or donkey anti-mouse Alexa 549 (1:200; Invitrogen) with horse biotinylated anti-mouse (1:200; Vector Laboratories) or goat biotinylated anti-rabbit (1:200; Vector Laboratories) antibodies followed by streptavidin Alexa 488 (1:1,000; Invitrogen), or with goat anti-guinea pig (1:200; Invitrogen), goat anti-rabbit (1:200; Invitrogen), or donkey anti-mouse (1:200; Invitrogen) antibodies conjugated with Alexa 488 or Alexa 647, and mounted in vectashield medium with DAPI (Vector Laboratories).

For GFP labeling, brain sections were incubated 2 min in proteinase K (Euromedex), rinsed for 1 h in glycine, saturated in blocking solution, and incubated for 48–72 h at 4 °C with a rabbit anti-GFP (1:5,000; Invitrogen). Sections were then incubated 2 h at room temperature in goat anti-rabbit (1:500; Invitrogen) antibodies conjugated with Alexa 488 and mounted in vectashield medium with DAPI (Vector Laboratories).

Quantification and Image Analysis. All cell counts were conducted by an experimenter blind to the genotype and experimental condition.

BrdU$^+$ nuclei quantification. Labeled profiles were counted with an Olympus microscope (BX60) coupled with mapping software (Mercator Pro; Explora Nova). All BrdU nuclei were counted in the DG of the hippocampus in eight sections per animal spaced by 280 μm, from bregma −1.34 mm to −3.28 mm, as previously described (4). For the OB, BrdU nuclei were counted in 12 sections spaced by 120 μm in the granule cell area including the mitral cell and internal plexiform layers. Immunostained nuclei for the SVZ were quantified in 50 × 50-μm areas and analyzed on 11 sections per animal spaced by 120 μm. The profile density (number of labeled cells per square millimeter on sections) was derived from these data, the volume of the region of interest was calculated according to conventional stereological equation, and the total number of cells was calculated as described previously (4).

NeuN$^+$, zif268$^+$ and c-Fos$^+$ cells quantification. To estimate the total number of mature NeuN neurons in the DG, six stacks in two sections per mouse (three of each DG blade) were collected at 40× using a confocal microscope (Zeiss LSM700). The number of NeuN$^+$/DAPI$^+$ cells in each stack was counted manually and the size of the counted area was measured. From this the density of NeuN$^+$ cells in the DG was calculated (5). For Zif268 or c-Fos, all positive nuclei were counted in three sections per animal spaced by 560 μm with an optical microscope coupled with mapping software (Mercator Pro). We then determined the proportion of mature NeuN neurons expressing Zif268 or c-Fos for each genotype and experimental condition as previously described (5).

Double- and triple-labeling analysis and quantification. Sections were analyzed using the Zeiss confocal system. To establish the percentage of BrdU cells double-labeled with DCX, NeuN, Zif268, GFAP, ACIII, GluR1, KCC2b, or NKCC1, or triple-labeled with NeuN and c-Fos or Zif268, 8–16 serial sections (280-μm spacing) from all mice were examined throughout the DG. Colocalizations were evaluated on 80–100 BrdU$^+$ cells per group of mice by performing *z*-stack acquisitions and 3D reconstructions to univocally verify double or triple labeling. All acquisitions were carried out in sequential scanning mode to prevent cross-bleeding between channels.

Statistical Analysis. All data were averaged across animals within each experimental group and are presented as means ± SE. Statistical comparisons were conducted by two-way ANOVA and by *t* test. Significance level was set at $P < 0.05$.

Analyses of GFP$^+$ Neurons. Images were acquired on a Zeiss confocal microscope. The *z*-stack series of confocal images were acquired at 1,024 × 1,024-pixel resolution, with a pinhole setting of one Airy unit and optimal settings for gain and offset. For dendritic analysis, 3D reconstructions of the dendritic processes of each GFP$^+$ neuron were made from *z*-stacks with a 40× objective. Lateral and *z*-axis resolutions were 280–350 nm and 500 nm, respectively. For spine density, dendrites were imaged through a 63× objective with lateral and *z*-axis resolutions of 50–80 nm and 200 nm, respectively. Dendritic processes and dendritic spines were then analyzed using NeuronStudio software. Total dendritic length, mean dendritic length, primary dendrite length, maximum and minimum dendrite length, and branching points of each individual GFP$^+$ neuron in the granule cell layer were analyzed. The Sholl analysis for dendritic complexity was carried out by counting the number of dendrites that cross a series of concentric circles at 20-μm intervals from the soma. These analyses were performed in 18–25 cells and 18–25 dendrites per group of mice. Data of dendritic length, branching points and spine density were compared between *zif268*-KO and WT mice using Student *t* test. Statistical comparisons for Sholl analysis were conducted by repeated measures two-way ANOVA followed by Student post hoc *t*-test. The statistical significance of cumulative frequency was assessed using Kolmogorov–Smirnov test.

1. Jones MW, et al. (2001) A requirement for the immediate early gene Zif268 in the expression of late LTP and long-term memories. *Nat Neurosci* 4(3):289–296.
2. Trouche S, Bontempi B, Roullet P, Rampon C (2009) Recruitment of adult-generated neurons into functional hippocampal networks contributes to updating and strengthening of spatial memory. *Proc Natl Acad Sci USA* 106(14):5919–5924.
3. van Praag H, et al. (2002) Functional neurogenesis in the adult hippocampus. *Nature* 415(6875):1030–1034.
4. Veyrac A, et al. (2011) CRMP5 regulates generation and survival of newborn neurons in olfactory and hippocampal neurogenic areas of the adult mouse brain. *PLoS One* 6:e23721.
5. Kee N, Teixeira CM, Wang AH, Frankland PW (2007) Preferential incorporation of adult-generated granule cells into spatial memory networks in the dentate gyrus. *Nat Neurosci* 10(3):355–362.

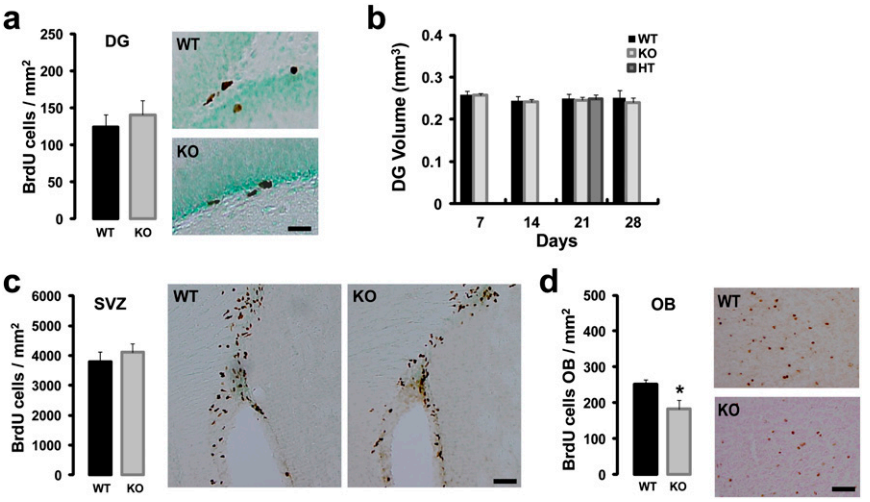

Fig. S1. Cell proliferation in the DG and SVZ and newborn neurons survival in the OB of WT and *zif268*-KO mice. (*A*) The total number of BrdU-labeled cells in the DG 4 h after one BrdU injection was similar between WT and *zif268*-KO mice. Number of mice: WT $n = 7$; KO $n = 7$. (Scale bar, 20 μm.) (*B*) The volume of the DG was similar between WT, HET, and *zif268*-KO mice. Number of mice: 7 d postinjection (dpi) 7 WT, 8 KO; 14 dpi 8 WT, 8 KO; 21 dpi 6 WT, 7 KO; 28 dpi 7 WT, 7 KO; 34 and 43 dpi 6 WT, 6 KO; (HET): 21 dpi $n = 5$. (*C*) No difference in proliferation of progenitor cells labeled with BrdU in SVZ between genotypes. Number of mice: WT $n = 7$; KO $n = 5$. (Scale bar, 100 μm.) (*D*) The total number of 21-d-old newborn cells is decreased in olfactory bulb of *zif268*-KO mice. (Scale bar, 50 μm.) Number of mice: WT $n = 6$; KO $n = 5$. Data are means ± SEM in this and subsequent figures. $^{*}P < 0.05$.

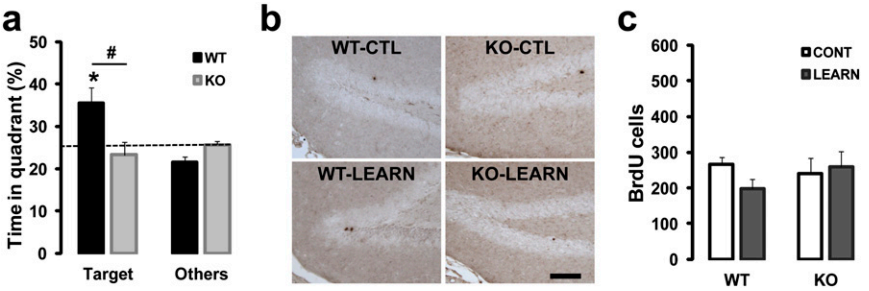

Fig. S2. Massed spatial training does not increase survival of 9-d-old newborn dentate granule cells (DGCs). (*A*) During the probe test 25 d after acquisition, WT mice spent significantly more time searching in the target quadrant compared with other quadrants, unlike *zif268*-KO mice that did not. WT, $n = 6$; KO, $n = 5$. (*B*) Photomicrographs showing BrdU staining in WT and *zif268*-KO mice at 34 dpi, 25 d after acquisition, in control (CTL) and learning (LEARN) groups. (Scale bar, 80 μm.) (*C*) No difference in the total number of $BrdU^{+}$ cells, aged 9 d at the time of acquisition, in the CTL and LEARN groups between genotypes. CTL and LEARN: WT $n = 6$; KO $n = 6$. $^{*}P < 0.05$, $^{\#}P < 0.05$.

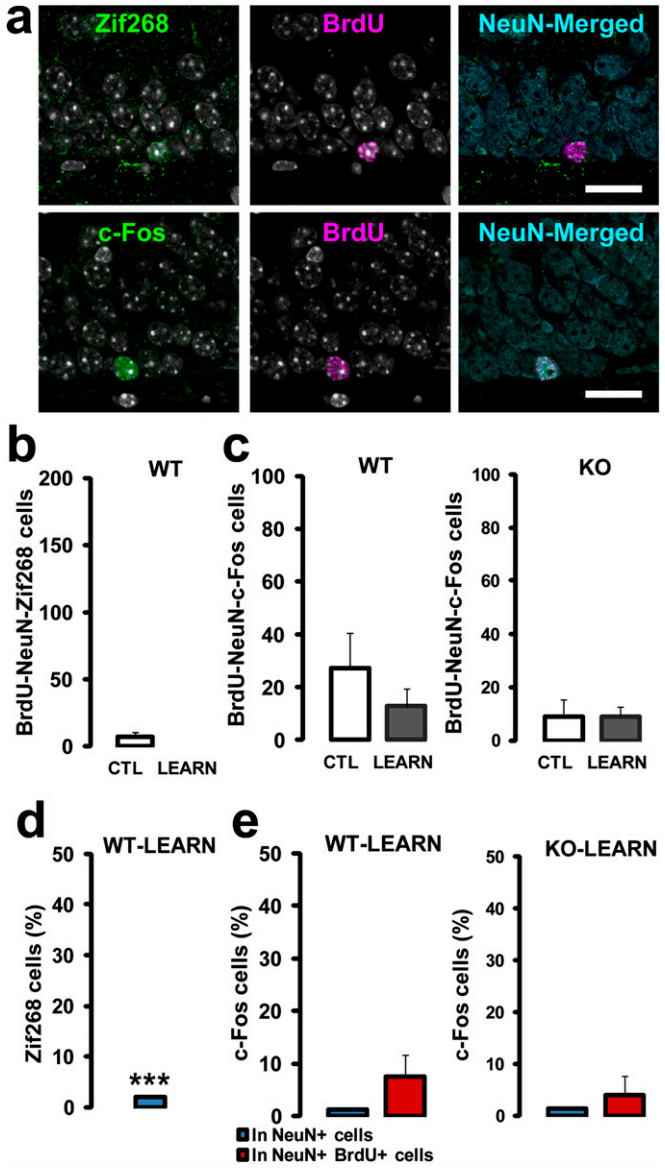

Fig. S3. Spatial training does not recruit 9-d-old newborn DGCs. (*A*) Confocal micrographs of 34-d-old $BrdU^+/NeuN^+$ neurons expressing Zif268 or c-Fos in a WT mouse. (Scale bar, 25 μm.) (*B*) Upon spatial memory recall (LEARN), the number of 9-d-old $BrdU^+/NeuN^+$ DGCs expressing Zif268 was not different from the control group (CTL). (*C*) The number of $BrdU^+/NeuN^+$ neurons expressing c-Fos upon recall was similar between genotypes and not significantly different from their respective control groups. (*D*) Upon recall, a higher proportion of preexisting neurons in WT mice expressed Zif268, compared with 9-d-old newborn DGCs. (*E*) The proportion of c-Fos–expressing neurons was similar for newborn and preexisting DGCs in WT mice and *zif268*-KO mice. CTL: WT $n = 6$; KO $n = 6$; LEARN: WT n= 5; KO $n = 6$. ***$P < 0.005$.

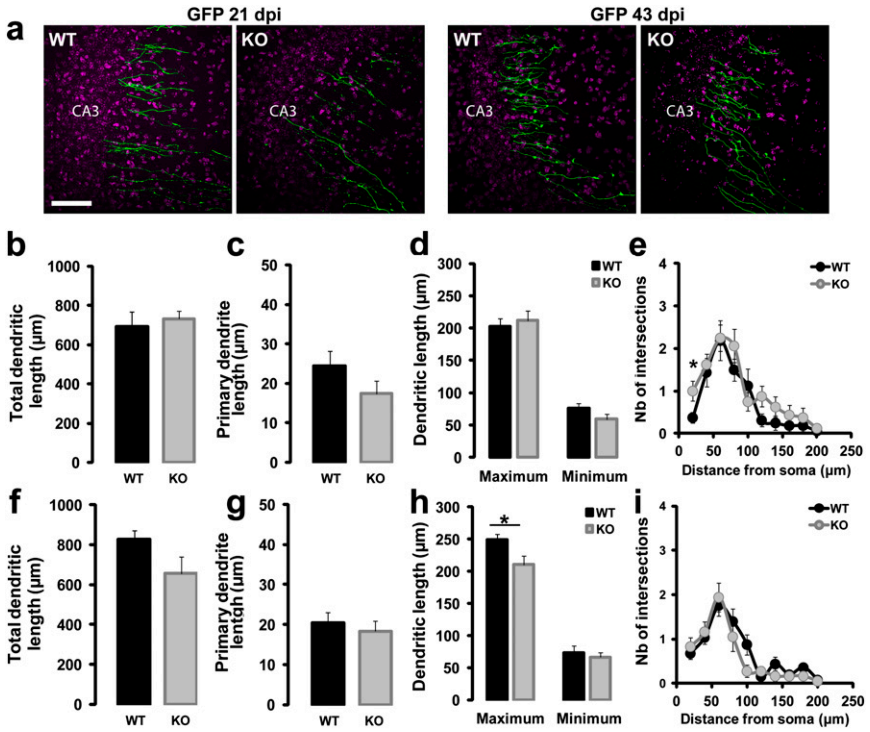

Fig. S4. *Zif268* regulates the morphological maturation of newborn neurons. (*A*) Confocal 3D reconstruction of axonal projections of newborn GFP-labeled DGCs in area CA3, 21 and 43 d after retroviral vector injection showing normal efferent connectivity in WT and *zif268*-KO mice. (Scale bar, 50 µm.) (*B*) Total dendrite length of 21-d-old newborn DGCs was similar between genotypes. (*C*) Primary dendrite length at 21 dpi was similar between genotypes. (*D*) Maximum and minimum length at 21 dpi was similar between WT and *zif268*-KO mice. (*E*) Sholl analysis of dendrite complexity at 21 dpi, showing more intersections near the soma in *zif268*-KO mice. (*F*) Total dendrite length at 43 dpi was similar between genotypes. (*G*) Primary dendrite length at 43 dpi was similar between genotypes. (*H*) Maximum length of dendrite of new DGCs aged 43 d is decreased in *zif268*-KO compared with WT mice. (*I*) Dendrite complexity at 43 dpi was similar between WT and *zif268*-KO mice. WT $n = 16$; KO $n = 16$ in *B–E*; WT $n = 25$; KO $n = 18$ in *F–I*. $^*P < 0.05$.

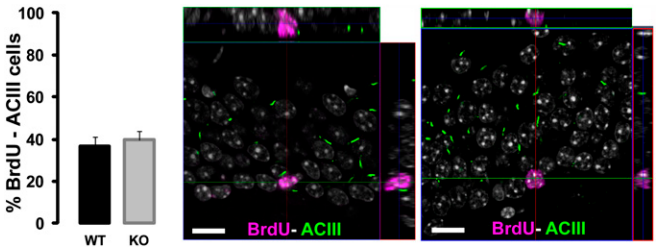

Fig. S5. *Zif268* is not required for primary cilia formation. The proportion of $BrdU^+/ACIII^+$ at 21 dpi was similar between genotypes. Representative $BrdU^+$ cell labeled (*Left*) or not labeled (*Right*) with ACIII. (Scale bars, 20 µm.) WT $n = 6$; KO $n = 7$.

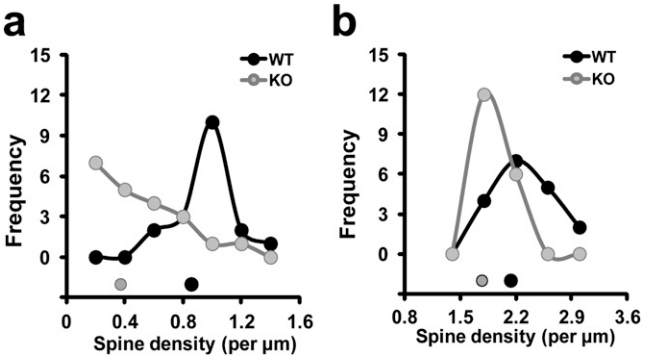

Fig. S6. *Zif268* regulates spine formation across the whole population of newborn DGCs. (*A*). Frequency of spine density in 21-d-old newborn DGCs. (*B*) Frequency of spine density in 43-d-old newborn DGCs. 21 dpi: WT $n = 16$; KO $n = 16$; 43 dpi: WT $n = 25$; KO $n = 18$.

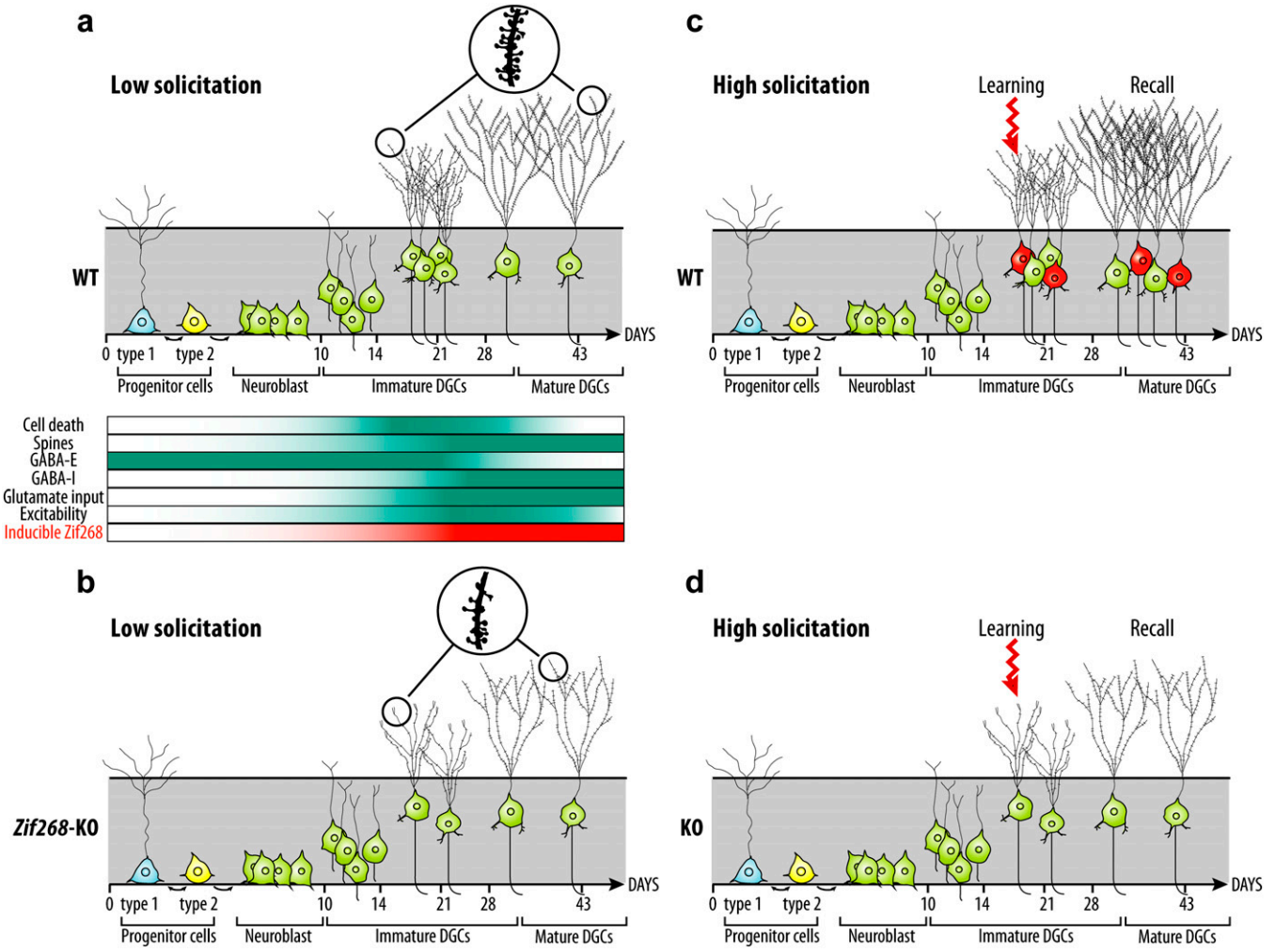

Fig. S7. Schematic model of *zif268* function in adult DG neurogenesis. (*Left*) Basal condition with low solicitation. (*A*) In WT mice, newborn DGCs (green), which derived from neural progenitors cells (type 1 and type 2, blue and yellow, respectively), migrate and integrate into the DG circuit within 6 wk after birth. Axons are elongated and contact hilar and CA3 pyramidal cells after 1–2 wk, then dendrites extend in the molecular layer and spines start to appear after 2 wk. During synaptogenesis, new DGCs compete to survive, leaving the majority eliminated by programmed cell death within 2–4 wk after birth. The physiological properties of newborn DGCs are marked by a gradual change in the expression of chloride cotransporters during the maturation processes. Before 21 d, immature neurons are initially depolarized by GABA (GABA-E) and then depolarized (GABA-I) along with expression of AMPA glutamate receptors and their progressive responsiveness to glutamatergic inputs. At this stage, newborn DGCs are hyperexcitable, display properties of enhanced synaptic plasticity, and are prone to integrate the exiting hippocampal neurocircuitry. In basal condition, a small proportion of newborn DGCs express Zif268 in an inducible manner. Inducible Zif268 expression significantly increases after 21 d, a period during which DGCs are selected to die or to survive for long-term functional integration. (*B*) In the absence of *zif268*, because of their neurochemical and morphological (zoom) delayed maturation, the selection of DGCs is drastically accelerated between 14 and 21 d after birth without affecting the whole population of surviving DGCs at longer delays. (*Right*) Condition of DG high solicitation. (*C*) In WT mice, the occurrence of spatial learning would recruit a population of newborn DGCs that are at the brink of selection during the critical period (red neurons, learning), as derived from their observed activation upon memory reactivation (red neurons, recall). As young newborn DGCs are activated by learning, they would express *zif268* and other immediately early genes and (yet unknown) gene programs, resulting in learning promoting their survival and functional incorporation into hippocampal network, thereby subserving long-term hippocampal-dependent memory formation. (*D*) In contrast, in the absence of *zif268*, young newborn DGCs (around 18-d-old) are functionally more immature. They are not recruited by learning and are not incorporated nor activated upon recall in association with impaired long-term memory. Image courtesy of Lydie Collet.